Published in final edited form as:
Neuroscience. 2009 December 15; 164(3): 1009–1019. doi:10.1016/j.neuroscience.2009.09.013.

Regulation of glutamatergic and GABAergic neurotransmission in the chick nucleus laminaris: role of N-type calcium channels

Yong Lu*
Department of Anatomy and Neurobiology, Northeastern Ohio Universities Colleges of Medicine and Pharmacy, 4209 State Route 44, PO Box 95, Rootstown, OH 44272

Abstract

Neurons in the chicken nucleus laminaris (NL), the third-order auditory nucleus involved in azimuth sound localization, receive bilaterally segregated (ipsilateral vs. contralateral) glutamatergic excitation from the cochlear nucleus magnocellularis and GABAergic inhibition from the ipsilateral superior olivary nucleus. Here, I investigate the voltage-gated calcium channels (VGCCs) that trigger the excitatory and the inhibitory transmission in the NL. Whole-cell recordings were performed in acute brainstem slices. The excitatory transmission was predominantly mediated by N-type VGCCs, as the specific N-type blocker ω-Conotoxin-GVIA (1-2.5 μM) inhibited excitatory postsynaptic currents (EPSCs) by ~90%. Blockers for P/Q- and L-type VGCCs produced no inhibition, and blockade of R-type VGCCs produced a small inhibition. In individual cells, the effect of each VGCC blocker on the EPSC elicited by activation of the ipsilateral input was the same as that on the EPSC elicited by activation of the contralateral input, and the two EPSCs had similar kinetics, suggesting physiological symmetry between the two glutamatergic inputs to single NL neurons. The inhibitory transmission in NL neurons was almost exclusively mediated by N-type VGCCs, as ω-Conotoxin-GVIA (1 μM) produced a ~90% reduction of inhibitory postsynaptic currents, whereas blockers for other VGCCs produced no inhibition. In conclusion, N-type VGCCs play a dominant role in triggering both the excitatory and the inhibitory transmission in the NL, and the presynaptic VGCCs that mediate the two bilaterally segregated glutamatergic inputs to individual NL neurons are identical. These features may play a role in optimizing coincidence detection in NL neurons.

Keywords

voltage-gated calcium channel; excitatory postsynaptic current; inhibitory postsynaptic current; coincidence detection; sound localization

Introduction

Calcium entry through voltage-gated calcium channels (VGCCs) is essential for triggering transmitter release at synaptic terminals. VGCCs are classified into multiple types based on their amino acid sequences, biophysics, and pharmacological properties. The alphabetical nomenclature of these channels (P/Q, N, R, L, and T) corresponds to $Ca_v2.1$, $Ca_v2.2$, $Ca_v2.3$, $Ca_v1.1$-1.4, and $Ca_v3.1$-3.3, respectively, which are VGCC members that have been

*Correspondence to: Yong Lu at the above address, Telephone: 330-325-6656, Facsimile: 330-325-5916, ylu@neoucom.edu.
Section Editor: Dr. Menahem Segal

characterized in mammals (review in Jones, 2003; Catterall et al., 2005). For the purpose of comparison, the alphabetical nomenclature is used here. The different types of VGCCs possess differential biophysical characteristics, and execute different cellular functions depending on their location in various cellular compartments. The main types that mediate chemical transmission at central nervous system (CNS) synapses are the P/Q- and N-types (Review in Jones, 2003; Reid et al., 2003), which differ in their activation voltage, spatial distribution at synapses, sensitivity to modulation, and channel open probability when inhibited (see Discussion for detail).

Interaural time difference is one of the major cues used by animals to localize sound source on the azimuth plane. The medial superior olive and the nucleus laminaris (NL) are the first central auditory nucleus that encodes this information in mammals and birds, respectively. Neurons in the NL receive bilaterally segregated excitatory inputs that are mediated by glutamate from the cochlear nucleus magnocellularis (NM), with inputs from the ipsilateral NM impinging onto the dorsal dendrites, and inputs from the contralateral NM onto the ventral dendrites (Parks and Rubel, 1975). NL neurons function as coincidence detectors that detect the convergent excitatory inputs from the two ears and generate information for azimuth sound localization (Young and Rubel, 1983; Overholt et al., 1992; Hyson, 2005). Neurons in the NL also receive an unusually depolarizing inhibitory input mediated by GABA from the ipsilateral superior olivary nucleus (SON) (Lachica et al., 1994; Yang et al., 1999; Burger et al., 2005). Despite the importance and variation of VGCCs in triggering synaptic transmission, the specific VGCC types that mediate the excitatory and the inhibitory inputs in the NL remain unknown. Therefore, the primary goal of this study was to characterize the VGCCs that trigger the excitatory and the inhibitory transmission in the NL.

Another aim of this study was to compare the two segregated glutamatergic inputs that impinge upon the same NL neuron. The bilateral dendrites of NL neurons are morphologically symmetrical (Parks and Rubel, 1975), implying physiological symmetry (balanced synaptic strength along the dorsal vs. the ventral dendrites) between the two segregated excitatory inputs. Indeed, NL neurons show similar thresholds to tone-burst stimulation presented to either ear (Rubel and Parks, 1975; Köppl and Carr 2008), suggesting that they have approximately equal sensitivity to either input. The importance of balanced excitatory inputs to the coincidence detectors can also be inferred from modeling studies, in which the same membrane parameters are assigned to the two excitatory inputs (Agmon-Snir et al., 1998; Grau-Serrat et al., 2003; Dasika et al., 2007). To date, however, there is a lack of quantitative experimental evidence that demonstrates the physiological symmetry of the two inputs at the cellular level. This study serves as an initial attempt to address this issue by testing the hypotheses that the VGCCs triggering glutamate release from the ipsilateral NM (i.e., the dorsal input) are the same as those from the contralateral NM (i.e., the ventral input), and that the two segregated excitatory inputs are symmetrical in terms of excitatory postsynaptic current (EPSC) kinetics.

Experimental Procedures

Slice preparation and in vitro whole-cell recordings

Fertilized chicken eggs (*Gallus domesticus*) were purchased from Purdue University (West Lafayette, IN) and incubated using an RX2 Auto Turner (Lyon Electric Co., Chula Vista, CA). Brainstem slices (250-300 μm in thickness) were prepared from late embryos (E18-E21) and early hatchlings (P6-P9) as previously described (Reyes et al., 1994; Tang et al., 2009), with modification of the artificial cerebrospinal fluid (ACSF) components used for dissection and cutting of the brain tissue. The modified ACSF, which is a glycerol-based solution (Ye et al., 2006), contained (in mM): 250 glycerol, 3 KCl, 1.2 KH_2PO_4, 20 $NaHCO_3$, 3 HEPES, 1.2 $CaCl_2$, 5 $MgCl_2$ and 10 dextrose, pH 7.4 when gassed with 95% O_2 and 5% CO_2. The procedures were approved by the Institutional Animal Care and Use Committee (IACUC) at

Northeastern Ohio Universities Colleges of Medicine and Pharmacy, and are in accordance with NIH policies on animal use. Slices were incubated for at least 1 hr in normal ACSF containing (in mM): 130 NaCl, 26 $NaHCO_3$, 3 KCl, 3 $CaCl_2$, 1 $MgCl_2$, 1.25 NaH_2PO_4 and 10 dextrose. The ACSF was constantly gassed with 95% O_2 and 5% CO_2 (pH 7.4).

For recording, slices were transferred to a 0.5 ml chamber mounted on a Zeiss Axioskop 2 FS Plus (Zeiss, Germany) with a 40× water-immersion objective and infrared, differential interference contrast optics. The chamber was continuously superfused with ACSF (1-2 ml/min) by gravity. The microscope was positioned on the top center of an Isolator CleanTop II and housed inside a Type II Faraday cage (Technical Manufacturing Corporation, Peabody, MA). Voltage clamp experiments were performed with an Axopatch 200B amplifier while current clamp experiments were performed with an Axoclamp 2B amplifier (Molecular Devices, Union City, CA). The voltage clamp experiments were performed at room temperature (20-22 °C). In these experiments, the peak amplitudes of the postsynaptic currents recorded under the control and experimental (VGCC blocker) conditions were compared, and the percent change in current amplitude was reported. Although exocytosis (transmitter release) is highly sensitive to temperature, the relative change in current amplitude due to the application of a VGCC blocker is presumably not affected by temperature. The current clamp experiments were performed at 34-36 °C, controlled by a Single Channel Temperature Controller TC324B (Warner Instruments, Hamden, CT). These experiments were performed under physiological temperature in order to minimize the influence of temperature on the temporal summation of the GABAergic responses.

Patch pipettes were drawn on an Electrode Puller PP-830 (Narishige, Japan) to 1-2 μm tip diameter using borosilicate glass Micropipets (inner diameter of 0.86 mm, outer diameter of 1.60 mm) (VWR Scientific, Seattle, WA). The electrodes had resistances between 3 and 7 MΩ when filled with an internal solution containing (in mM): 105 K-gluconate, 35 KCl, 5 EGTA, 10 HEPES, 1 $MgCl_2$, 4 ATP-Mg, and 0.3 GTP-Na, pH 7.2 (adjusted with KOH). The liquid junction potential was 10 mV, and data were corrected accordingly. Placement of the electrodes was controlled by a motorized micromanipulator MP-225 (Sutter Instrument, Novato, CA). Data were low-pass filtered at 3 or 5 kHz for current clamp and voltage clamp experiments, respectively, and digitized using a Data Acquisition Interface ITC-18 (Instrutech, Great Neck, NY) at 20 kHz. In each voltage clamp recording, cells were clamped at -60 mV, a value close to their resting membrane potential (RMP) (Gao and Lu, 2008). Cells recorded under the current clamp mode received no additional current injections, and thus recordings started at their RMP. The morphology of some recorded cells was revealed by adapting a method by Hamam and Kennedy (2003). Biocytin (0.1-0.5%) was added to the internal solution used for whole-cell recordings. After physiological recordings, brain slices were fixed overnight in 4% paraformaldehyde. Biocytin was visualized with avidin-biotin peroxidase and diaminobenzidine.

Synaptic stimulation and recordings—Extracellular synaptic stimulation was performed using concentric bipolar electrodes with a tip core diameter of 127 μm (World Precision Instruments, Sarasota, FL). Square electric pulses (duration of 200 μs) were delivered through a Stimulator A320RC (World Precision Instruments, Sarasota, FL). The stimulation electrode was placed using a Micromanipulator NMN-25 (Narishige, Japan). Cell bodies of NL neurons form a laminar structure in transverse tissue sections, and can be reliably identified under the microscope (Fig. 1A, B). To activate the two segregated glutamate pathways to the NL, two stimulation setups were used. One stimulation electrode was placed on the ipsilateral NM, and the other on the fiber tract ventral and medial to the NL, which originates from the contralateral NM. To activate the GABAergic pathway, a stimulation electrode was placed on the fiber tract lateral to the NL (Fig. 1C).

EPSCs were recorded in the presence of bicuculline (20 μM) or SR-95531 (gabazine, 10 μM), which are $GABA_A$ receptor antagonists. Inhibitory postsynaptic currents or potentials (IPSCs or IPSPs, respectively) were recorded in the presence of ionotropic glutamate receptor antagonists DNQX (50 μM) and APV (100 μM). QX 314 (5 mM), a sodium channel blocker, was included in the recording electrodes to prevent action currents. All chemicals and drugs were obtained from Sigma (Saint Louis, MO), except for SNX-482, ω-Conotoxin-GVIA (ω-CTx-GVIA) and tACPD, which were obtained from Peptide International (Louisville, KY), Alomone Labs (Jerusalem, Israel), and Tocris (Ballwin, MO), respectively. All drugs were bath-applied.

Consideration of selectivity of toxins/antagonists for VGCCs used in this study—Nimodipine (10 μM), ω-CTx-GVIA (1-2.5 μM), and ω-Agatoxin-IVA (ω-Aga-IVA, 100 nM) were used to block L-, N-, and P/Q-type VGCCs, respectively. Nimodipine (10 μM), a dihydropyridine compound, is a selective L-type Ca^{2+} channel blocker (McCarthy and TanPiengco, 1992; Randall and Tsien, 1995). ω-CTx-GVIA (1-2.5 μM), a cone snail toxin, irreversibly blocks N-type Ca^{2+} channels (Boland et al., 1994; Randall and Tsien, 1995). ω-Aga-IVA (100 nM) blocks P/Q-type Ca^{2+} channels, and the two components (P- and Q-type) are not further distinguished. Although a higher concentration (1 μM) of ω-Aga-IVA is needed to fully block P/Q-type channels while leaving N-type channels intact in bovine chromaffin cells (Albillos et al., 1993), the concentration used here (100 nM) was expected to relatively effectively block P/Q-type channels of chicken brainstem neurons, because a 3-fold increase in the concentration of the blocker does not produce further inhibition of calcium channels in neurons of the cochlear nucleus magnocellularis in the same kind of chicken brain slice preparations as used in the present study (Lu and Rubel, 2005). Specificities of ω-CTx-GVIA for N-type and ω-Aga-IVA for P/Q-type VGCCs are high, and interactions between them at the utilized concentrations are minimal (Sidach and Mintz, 2000; McDonough et al., 2002). The non-selective blockade of N-type channels by ω-Aga-IVA was found only at high concentrations (1 μM, 10 times higher than the concentration used in the present study) (Sidach and Mintz, 2000). Cytochrome c (0.5 mg/ml) was included in the ACSF used for the preparation of these two toxins in order to reduce non-specific binding. The effectiveness of these Ca^{2+} channel blockers on VGCCs of neurons in chicken brain slice preparations has been previously confirmed (Lu and Rubel, 2005).

R-type channel currents were initially defined as the resistant (hence the “R”) current in the presence of blockers for L-, N-, and P/Q-types (Randall and Tsien, 1995). SNX-482 was developed in 1998 as a potent and selective antagonist for R-type VGCCs (Newcomb et al., 1998). The selectivity of SNX-482, however, is highly dose-dependent. At a low concentration (20 nM), SNX-482 selectively blocks R-type VGCCs (Mergler et al., 2003). At high concentrations (>300 nM), non-specific blockade of other type VGCCs is observed (Arroyo et al., 2003; Urbano et al., 2003). The concentration of 50 nM used in this study was chosen as it is expected to be both effective and selective on R-type VGCCs.

Data analysis—Recording protocols were written and run using Axograph acquisition and analysis software, version 4.9 (Molecular Devices, Union City, CA). Peak values of EPSCs and IPSCs were measured from the baseline, which was zeroed at about 5-10 ms prior to the onset of the stimulus artifact. Statistical analysis was performed using Excel (Microsoft, Redmond, WA) and Statview (Abacus Concepts, Berkeley, CA), and graphs were constructed in Igor (Wavemetrics, Lake Oswego, OR). Statistical differences were detected using paired t-tests. Means and standard deviations are reported (n in parenthesis indicates the number of cells).

Results

Effects of Ca^{2+} channel blockers on the excitatory transmission in the NL

The dorsal and ventral glutamatergic pathways to the NL were activated by the delivery of two separate electrical stimulations using two stimulus setups (Fig. 1C), with an inter-stimulus interval of 75 ms. This interval is long enough to avoid any interactions between the two EPSCs, as responses elicited by the individual stimuli alone were the same as those elicited when both stimuli were presented at the interval of 75 ms (data not shown). Stimulus intensities were adjusted to give rise to EPSCs of approximately equal peak amplitude (close to the maximal amplitude). Each of the VGCC blockers was bath-applied for 4-10 min until a steady state current was obtained, followed by wash out of the drug. Glutamatergic transmission in the NL was primarily triggered by Ca^{2+} entry through N-type VGCCs (Fig. 2A). Little or no inhibition of EPSCs was observed when the P/Q-type blocker ω-Agatoxin-IVA (ω-Aga-IVA, 0.1 μM) or the L-type blocker nimodipine (10 μM) was applied (Fig. 2B, C). A small reversible inhibition by the R-type blocker SNX-482 (50 nM) was observed (Fig. 2D). The variable time courses of the EPSCs observed in different neurons may be due to the fact that neuronal properties of NL neurons are distributed along the tonotopic axis in a frequency-dependent manner, with the mid-frequency coding neurons having faster responses compared to the low- and high-frequency coding neurons (Kuba et al., 2005). Figure 2E shows that ω-CTx-GVIA inhibited the ipsilateral and the contralateral EPSCs by 88 ± 7% and 86 ± 13% (n = 9), respectively. Three of the nine cells were obtained in P8-9 chicks and showed no differences in terms of the effectiveness of ω-CTx-GVIA (1 μM) on EPSCs. Therefore, the data obtained from hatchlings were combined with those obtained from late embryos. In another NL neuron obtained from a P5 chick, a cocktail of non-N-type blockers (0.1 μM ω-Aga-IVA, 10 μM nimodipine, and 50 nM SNX-482) did not produce a noticeable inhibition of EPSCs (data not shown). SNX-482 (50 nM) produced a small inhibition with large variations among cells (ipsilateral: 20 ± 14%; contralateral: 16 ± 17%, n = 7). The large variations of the effects of SNX-482 on EPSCs were obviously noticeable when the percent change in EPSC amplitude was assessed in individual neurons (ipsilateral: 15, 28, 21, 40, 29, -3, and 7% reduction; contralateral: 13, 20, 8, 33, 44, 0, and -3% reduction), suggesting that different proportions, if any, of SNX-482-sensitive VGCCs participate in triggering glutamate release in different NL neurons. These large variations may well account for the seemingly puzzling observation described earlier, in which a cocktail of the VGCC blockers including SNX-482 did not inhibit EPSCs in the NL neuron obtained from the P5 chick. It is possible that the glutamatergic terminals innervating this neuron did not have SNX-482-sensitive VGCC. Blockers for P/Q- and L-type VGCCs had no effects on EPSCs. No statistical differences were found in the percentage of inhibition by the same blocker between the ipsilateral and the contralateral EPSCs (paired t-test, $p > 0.05$), indicating that the presynaptic VGCCs that mediate the two bilaterally segregated glutamatergic inputs to individual NL neurons are identical. The total percent inhibition by all four drugs on either the ipsilateral or the contralateral EPSCs slightly exceeded 100%. This result was expected, because the blockers were applied individually rather than sequentially to different cells.

Identical kinetics between the ipsilateral and the contralateral EPSCs

To further characterize the physiological symmetry between the ipsilateral and the contralateral excitatory inputs to the NL, I compared the time course of the ipsilateral EPSCs with that of the contralateral EPSCs recorded from the same cells. A paired t-test revealed no statistical differences between the ipsilateral and the contralateral EPSCs in their 10-90% rise time (ipsilateral: 0.56 ± 0.11 ms; contralateral: 0.58 ± 0.17 ms, n = 21) or decay time constant (ipsilateral: 1.46 ± 0.45 ms; contralateral: 1.46 ± 0.51 ms, n = 21) (Fig. 3). Therefore, the ipsilateral and the contralateral EPSCs in the same NL neuron had nearly identical kinetics. This conclusion, however, is dependent on the validity of the assumption that the electrical

stimulation eliciting the ipsilateral EPSC is independent of that eliciting the contralateral EPSC. If the two stimulations activated the same population of synapses, one would surely observe EPSCs of the same properties. Therefore, I confirmed this assumption by providing two additional pieces of evidence.

First, I intentionally adjusted the intensities of the electrical stimuli so that maximal responses were recorded, and the amplitude of the ipsilateral EPSC was about the same as that of the contralateral EPSC. Consequently, when the peak amplitude of the contralateral EPSC was plotted against that of the ipsilateral EPSC, the data points fell on or were very close to the line indicating equivalence (Fig. 4A). In contrast, the stimulation intensity eliciting the ipsilateral EPSC was substantially different from that eliciting the contralateral EPSC. When the stimulus intensity delivered to the contralateral pathway was plotted against that given to the ipsilateral pathway, the data points were scattered (Fig. 4B). This observation suggests that the responses elicited by the two stimulations were essentially independent.

The second piece of evidence was obtained by taking advantage of the profound synaptic depression of EPSCs in NL neurons (Fig. 4C), which has been shown to improve coincidence detection (Kuba et al., 2002b). Figure $4C_1$ shows that a disynaptic EPSC was occasionally observed in the recordings of the ipsilateral, but not the contralateral EPSCs (also see Fig. 2A, top traces). The disynaptic EPSC was likely due to activation of the auditory nerve terminals innervating the ipsilateral NM, which in turn sends excitatory projections to the NL. After obtaining ipsilateral EPSCs and contralateral EPSCs of approximately equal amplitude, a train of synaptic stimulation (100 Hz, 20 pulses) was applied to activate the input from the ipsilateral NM, followed by the same stimulus protocol delivered to activate the input from the contralateral NM to the NL. Ipsilateral EPSCs showed synaptic depression and some temporal summation (Fig. $4C_2$). In contrast, the contralateral EPSCs showed similar synaptic depression but little summation (Fig. $4C_3$). The differential temporal summation is probably not due to different EPSC kinetics. It is more likely that the disynaptic EPSC observed only in the ipsilateral recordings accounts for this phenomenon. Importantly, when the ipsilateral train stimulation was followed by the contralateral train stimulation, the contralateral EPSCs showed a similar profile of synaptic depression to that elicited by the contralateral train stimulation alone (Fig. $4C_4$), and vice versa (Fig. $4C_5$), strongly indicating that the two stimulations are independent.

Effects of Ca^{2+} channel blockers on the inhibitory transmission in the NL

Neurons in the NL receive depolarizing GABAergic inputs from the ipsilateral superior olivary nucleus (SON). To reveal which types of VGCCs trigger GABA release onto NL neurons, I studied the effects of VGCC blockers on the inhibitory postsynaptic currents (IPSCs). The GABAergic transmission in the NL was almost exclusively triggered by Ca^{2+} entry through N-type VGCCs (Fig. 5). The IPSCs were almost completely and irreversibly blocked by the N-type blocker ω-CTx-GVIA (1 μM) (Fig. 5A). Blockers of other VGCCs did not produce any apparent effects on IPSCs (Fig. 5B-D). Pooled data show that ω-CTx-GVIA reduced the IPSCs by 89 ± 11% (n = 8; Fig. 5E). Two out of the eight cells were obtained in P6 chicks and showed no differences in terms of the effectiveness of ω-CTx-GVIA (1 μM) on IPSCs. The data were therefore combined with those obtained from late embryos. From these results, I conclude that N-type VGCCs are the dominant type that mediates both the glutamatergic and the GABAergic transmission in NL neurons. This conclusion is also supported by data obtained in younger animals (E13, n = 2; data not shown).

GABAergic responses of NL neurons maintained a tonic feature when modulated

Due to an unusually high intracellular Cl^- concentration that persists into maturation in NL neurons, activation of the GABAergic pathway gives rise to membrane depolarization (Hyson

et al., 1995; Funabiki et al., 1998; Tang et al., 2009). Given the high spiking activity of SON neurons *in vivo* (spontaneous firing rate of 30-80 Hz) (Lachica et al., 1994; Nishino et al., 2008), a sustained membrane depolarization in NL neurons is likely to exist. Although depolarizing, the net effect of the GABAergic inputs is inhibitory (Monsivais and Rubel, 2001). The sustained GABA-mediated membrane depolarization (temporally summated IPSP) is critical to improve coincidence detection in the NL (Funabiki et al., 1998). We previously showed that presynaptic metabotropic glutamate and GABA receptors (mGluRs and $GABA_B$Rs) inhibit GABA release in the NL (Tang et al., 2009). I predicted that IPSPs in NL neurons maintain a tonic feature even when GABAergic transmission is under modulation. To test this hypothesis, I examined the effects of agonists for mGluRs and $GABA_B$Rs on the GABAergic responses (Fig. 6). A train of synaptic stimulation (duration of 500 ms) at different frequencies (10, 50, 100, or 200 Hz) was delivered to activate the GABAergic inputs. IPSPs with discrete peaks were observed during low frequency stimulation (10 Hz). Temporal summation of IPSPs occurred at higher frequencies, forming a plateau of membrane depolarization. Activation of either mGluRs by tACPD (100 μM, n = 7) or $GABA_B$Rs by baclofen (100 μM, n = 7) substantially reduced the amplitude of the IPSPs, but maintained a depolarization plateau during stimulation at high frequencies.

Discussion

The main finding of this study is that N-type VGCCs play a dominant role in triggering both the excitatory and the inhibitory transmission in NL neurons. Furthermore, I found that the same types of VGCCs mediate the ipsilateral and the contralateral glutamatergic transmission in individual NL neurons, and that the ipsilateral and the contralateral EPSCs have the same kinetics. Herein, I provide the first evidence at the cellular level of physiological symmetry between the two segregated glutamatergic inputs to individual NL neurons. Finally, when modulated by mGluRs or $GABA_B$Rs, the GABAergic inputs maintain a tonic influence on the membrane potential of NL neurons.

Comparisons with previous studies

Synaptic transmission in the CNS is primarily mediated by P/Q- and N-type VGCCs, while other channel types are involved in only a few systems (review in Jones, 2003; Reid et al., 2003). The presence of one type and not the other at certain synapses may be based on their particular function in neuronal circuits at different developmental stages. For example, multiple types of VGCCs trigger neurotransmission in the medial nucleus of trapezoid body (MNTB) during development, and the P/Q- type dominates after maturation (Iwasaki and Takahashi, 1998; Ishikawa et al., 2005; Inchauspe et al., 2007; but also see Wu et al., 1999). When P/Q-type channels in MNTB are genetically knocked out, there is a functional compensatory increase in the expression of N-type channels. Consequently, short-term plasticity indicators, such as the paired-pulse facilitation that is readily observed in wild type animals, are diminished, indicating that P/Q- but not N-type channels provide facilitatory drive at MNTB synapses (Inchauspe et al., 2004).

In the NL, GABA release was almost exclusively triggered by N-type channels, with no apparent contribution by other VGCCs (Fig. 5). Glutamatergic transmission in the NL was also primarily triggered by N-type channels, with a small contribution from R-type channels in a small fraction of NL neurons (Fig. 2). The involvement of the R-type channels in the NL is consistent with previous findings that this type of VGCC also mediates rapid transmitter release (Wu et al., 1998,1999). The significance of the involvement of R-type channels in fast neurotransmission is unknown. In the medial superior olive, the mammalian analog of the NL, glutamatergic transmission is mediated by both N- and P/Q-type VGCCs with similar contributions, and glycinergic transmission is mediated by both N- and P/Q-type VGCCs, with

the latter being more dominant (Barnes-Davies et al., 2001). Species differences may account for the discrepancy in VGCCs that mediate synaptic transmission between the MSO and the NL.

The dominant role of N-type channels in triggering synaptic transmission in the NL appears to persist into maturation. N-type channels are replaced by P/Q-type channels for the triggering of glutamate release in the MNTB at roughly the age of hearing onset in the rat, which occurs at about P11-15 (Iwasaki and Takahashi, 1998; but also see Wu et al., 1999, who demonstrated the presence of N-type channels at P10-14). Chickens are precocial animals, i.e., they are able to hear before they hatch, with an early onset of hearing (defined here as the time when evoked brainstem potentials in response to intense sound stimulation can be recorded) at about E11/12 (Saunders et al., 1973). A few days after the onset of hearing (at E16-19), the chicken auditory system is able to detect and encode ambient sound (Jones et al., 2006). In late chicken embryos (> E18), which were used in the current study, NL neurons have adult-like neuronal properties, including intrinsic membrane and synaptic properties (Kuba et al., 2002a; Gao and Lu, 2008). In addition, in days-old chicks (P6-9), which have been demonstrated to have a fairly mature hearing threshold and behavior (Gray and Rubel, 1985; Rubel and Parks, 1988; Manley et al., 1991), ω- CTx-GVIA (1 μM) produced a similar blockade of EPSCs (n = 3) and IPSCs (n = 2) to that found in late embryos (data combined and shown in Figs. 2 and 5, respectively). Unlike some systems in the mammalian CNS (Iwasaki et al., 2000), a developmental switch of VGCCs at the axonal terminals in the NL may not occur.

Dominant role of N-type VGCCs in synaptic transmission in the NL

There are four essential physiological differences between P/Q- and N-type VGCCs, and each of the differences may suit a particular function at different synapses (Colecraft et al., 2000, 2001; Inchauspe et al., 2004).

First, N-type channel currents require a greater positive activation voltage than P/Q-type channels. The half-activation voltage for N-type channels is seven mV more depolarized than that for P/Q-type channels (Ishikawa et al., 2005). Strong membrane depolarizations are therefore needed at the axonal terminals, where N-type channels dominate, to induce sufficient Ca^{2+} entry in order to trigger transmitter release. The requirement of strong membrane depolarizations for glutamate release may play a role in the NL, where spiking activity in response to monaural inputs must be minimized. Furthermore, the slope of the power relationship between the N-type currents and EPSCs is lower than that for the P/Q-type channels (Wu et al., 1999). Consequently, synaptic facilitation is not as frequently observed at synapses where N-type channels dominate (Currie and Fox, 2002; Urbano et al., 2003; Inchauspe et al., 2004, 2007). Indeed, synaptic facilitation is lacking in the NL, whereas synaptic depression, the form of short-term plasticity opposite to synaptic facilitation, is profound in NL neurons and has been shown to improve the accuracy of coincidence detection (Kuba et al., 2002b).

Second, N-type channels are less tightly coupled to synaptic vesicles and are located at distances farther from the transmitter release sites than are P/Q-type channels (Inchauspe et al., 2007), leading to a smaller quantal content at synapses where N-type channels dominate. Thus, in order to elicit suprathreshold excitatory postsynaptic potentials in either the dorsal or ventral input in NL neurons, multiple glutamate release sites may need to be activated simultaneously (monaural coincidence detection), helping to minimize spiking activity of NL neurons in response to monaural inputs.

Third, N-type channels are preferentially subject to greater modulation by G-protein-coupled receptors (GPCRs) because they are more tightly linked to heterotrimeric G-proteins than are P/Q-type channels (review in Reid et al., 2003). Interestingly, the GABAergic, but not the

glutamatergic transmission in the NL, is subject to modulation by presynaptic $GABA_B$Rs and mGluRs (Tang et al., 2009). This selective modulation, however, is probably not due to differential VGCCs that mediate the release of GABA and glutamate in the NL, because N-type channels trigger both GABA and glutamate release in this nucleus. Elucidation of the mechanisms that underlie this selective modulation awaits further investigation.

Finally, when modulated by GPCRs, N-type channels remain available to be activated, whereas P/Q-type channels show little or no activation (Colecraft et al., 2000, 2001). When modulated (mainly inhibited) by GPCRs, VGCCs alter their activation status from a “willing” (normal) mode to a “reluctant” (inhibited) mode (Bean, 1989; Patil et al., 1996). As the terms indicate, in the willing mode, channels can open in response to membrane depolarization, whereas in the reluctant mode, it is more difficult to induce channel opening. Interestingly, there is a different level of “reluctance” for different channels. Using single-channel recordings, Colecraft et al. (2001) provided direct evidence that P/Q-type channels, when inhibited, become truly and completely reluctant, with no channel openings observed in response to membrane depolarizations. In contrast, N-type channels, when in the reluctant mode, are able to open in response to membrane depolarizations, only their open probability is lower than when they are in the willing mode. Therefore, at axonal terminals where N-type channels dominate, transmitter release is not likely to be shut down by inhibitory GPCRs. Along with the relatively slow kinetics of $GABA_A$R responses and the association of N-type channels with asynchronous release of GABA, activation of N-type channels even if when they are in the reluctant mode may contribute to the sustained depolarizing inhibitory action of GABA in the NL. The sustained feature is critical for the GABAergic input to exert its physiological action on coincidence detection in the NL (Funabiki et al., 1998). Taken together, the dominance of N-type VGCCs in triggering both the excitatory and the inhibitory transmission in the NL may play an important role in improving the acuity of temporal processing of sounds in the auditory brainstem.

Acknowledgments

This work was supported by Northeastern Ohio Universities Colleges of Medicine and Pharmacy startup funds, and the National Institute on Deafness and other Communication Disorders Grant R01 DC008984 to YL. The author thanks Dr. Hongxiang Gao for technical assistance, Ms. Susan Motts and Dr. Kyle Nakamoto for taking the photographs presented in Figure 1, and Dr. Zheng-Quan Tang and the anonymous reviewer for critical comments on an earlier version of the manuscript.

Abbreviations

ACSF	artificial cerebrospinal fluid
ω-Aga-IVA	ω-Agatoxin-IVA
CNS	central nervous system
ω-CTx-GVIA	ω-Conotoxin-GVIA
EPSC	excitatory postsynaptic current
$GABA_B$R	gamma-aminobutyric acid B receptor
GPCR	G-protein-coupled receptor
IPSC	inhibitory postsynaptic current
IPSP	inhibitory postsynaptic potential
mGluR	metabotropic glutamate receptor

MNTB	medial nucleus of trapezoid body
NL	nucleus laminaris
NM	nucleus magnocellularis
SON	superior olivary nucleus
VGCC	voltage-gated calcium channel

References

Agmon-Snir H, Carr CE, Rinzel J. The role of dendrites in auditory coincidence detection. Nature 1998;393:268–272. [PubMed: 9607764]

Albillos A, Garcia AG, Gandia L. ω-Agatoxin-IVA-sensitive calcium channels in bovine chromaffin cells. FEBS 1993;336:259–262.

Arroyo G, Aldea M, Fuentealba J, Albillos A, Garcia AG. SNX482 selectively blocks P/Q Ca^{2+} channels and delays the inactivation of Na^{+} channels of chromaffin cells. Eur J Phamacol 2003;475:11–18.

Barnes-Davis M, Owens S, Forsythe ID. Calcium channels triggering transmitter release in the rat medial superior olive. Hear Res 2001;162:134–145. [PubMed: 11707360]

Bean BP. Neurotransmitter inhibition of neuronal calcium currents by changes in channel voltage dependence. Nature 1989;340(6229):153–156. [PubMed: 2567963]

Boland LM, Morrill JA, Bean BP. omega-Conotoxin block of N-type calcium channels in frog and rat sympathetic neurons. J Neurosci 1994;14(8):5011–5027. [PubMed: 8046465]

Burger RM, Cramer KS, Pfeiffer JD, Rubel EW. The avian superior olivary nucleus provides divergent inhibitory input to parallel auditory pathways. J Comp Neurol 2005;481:6–18. [PubMed: 15558730]

Catterall WA, Perez-Reyes E, Snutch TP, Striessnig J. International union of pharmacology. XLVIII. Nomenclature and structure-function relationships of voltage-gated calcium channels. Pharmacol Rev 2005;57:411–425. [PubMed: 16382099]

Colecraft HM, Brody DL, Yue DT. G-protein inhibition of N- and P/Q-type calcium channels: distinctive elementary mechanisms and their functional impact. J Neurosci 2001;21(4):1137–1147. [PubMed: 11160384]

Colecraft HM, Patil PG, Yue DT. Differential occurrence of reluctant openings in G-protein-inhibited N- and P/Q-type calcium channels. J Gen Physiol 2000;115:175–192. [PubMed: 10653895]

Currie KP, Fox AP. Differential facilitation of N- and P/Q-type calcium channels during trains of action potential-like waveforms. J Physiol 2001;539(2):419–431. [PubMed: 11882675]

Dasika VK, White JA, Colburn HS. Simple models show the general advantages of dendrites in coincidence detection. J Neurophysiol 2007;97:3449–3459. [PubMed: 16914612]

Funabiki K, Koyano K, Ohmori H. The role of GABAergic inputs for coincidence detection in the neurones of nucleus laminaris of the chick. J Physiol 1998;508(3):851–869. [PubMed: 9518738]

Gao H, Lu Y. Early development of intrinsic and synaptic properties in chicken nucleus laminaris neurons. Neuroscience 2008;153:131–143. [PubMed: 18355968]

Grau-Serrat V, Carr CE, Simon JZ. Modeling coincidence detection in nucleus laminaris. Biol Cybern 2003;89:388–396. [PubMed: 14669019]

Gray L, Rubel EW. Development of absolute thresholds in chickens. J Acoust Soc Am 1985;77(3):1162–1172. [PubMed: 3980868]

Hamam BN, Kennedy TE. Visualization of the dendritic arbor of neurons in intact 500 μm thick brain slices. J Neurosci Methods 2003;123:61–67. [PubMed: 12581850]

Hyson RL. The analysis of interaural time differences in the chick brain stem. Physiol Behav 2005;86(3):297–305. [PubMed: 16202434]

Hyson RL, Reyes AD, Rubel EW. A depolarizing inhibitory response to GABA in brainstem auditory neurons of the chick. Brain Res 1995;677:117–126. [PubMed: 7606455]

Inchauspe CG, Forsythe ID, Uchitel OD. Changes in synaptic transmission properties due to the expression of N-type calcium channels at the calyx of Held synapse of mice lacking P/Q-type calcium channels. J Physiol 2007;584(3):835–851. [PubMed: 17823210]

Inchauspe CG, Martini FJ, Forsythe ID, Uchitel OD. Functional compensation of P/Q by N-type channels blocks short-term plasticity at the calyx of Held presynaptic terminal. J Neurosci 2004;24(46):10379–10383. [PubMed: 15548652]

Ishikawa T, Kaneko M, Shin H, Takahashi T. Presynaptic N-type and P/Q-type Ca^{2+} channels mediating synaptic transmission at the calyx of Held of mice. J Physiol 2005;568(1):199–209. [PubMed: 16037093]

Iwasaki S, Takahashi T. Developmental changes in calcium channel types mediating synaptic transmission in rat auditory brainstem. J Physiol 1998;509(2):419–423. [PubMed: 9575291]

Iwasaki S, Momiyama A, Uchitel OD, Takahashi T. Developmental changes in calcium channel types mediating central synaptic transmission. J Neurosci 2000;20(1):59–65. [PubMed: 10627581]

Jones SW. Calcium channels: unanswered questions. J Bioenerg Biomembr 2003;35(6):461–475. [PubMed: 15000516]

Jones TA, Jones SM, Paggett KC. Emergence of hearing in the chicken embryo. J Neurophysiol 2006;96:128–141. [PubMed: 16598067]

Köppl C, Carr CE. Maps of interaural time difference in the chicken's brainstem nucleus laminaris. Biol Cybern 2008;98:541–559. [PubMed: 18491165]

Kuba H, Koyano K, Ohmori H. Development of membrane conductance improves coincidence detection in the nucleus laminaris of the chicken. J Physiol 2002a;540(Pt 2):529–542. [PubMed: 11956341]

Kuba H, Koyano K, Ohmori H. Synaptic depression improves coincidence detection in the nucleus laminaris in brainstem slices of the chick embryo. Eur J Neurosci 2002b;15:984–990. [PubMed: 11918658]

Kuba H, Yamada R, Fukui I, Ohmori H. Tonotopic specialization of auditory coincidence detection in nucleus laminaris of the chick. J Neurosci 2005;25(8):1924–1934. [PubMed: 15728832]

Lachica EA, Rübsamen R, Rubel EW. GABAergic terminals in nucleus magnocellularis and laminaris originate from the superior olivary nucleus. J Comp Neurol 1994;348:403–418. [PubMed: 7844255]

Lu Y, Rubel EW. Activation of metabotropic glutamate receptors inhibits high voltage-gated calcium channel currents in chicken nucleus magnocellularis neurons. J Neurophysiol 2005;93:1418–1428. [PubMed: 15371493]

Manley GA, Kaiser A, Brix J, Gleich O. Activity patterns of primary auditory-fibers in chickens: development of fundamental properties. Hear Res 1991;57:1–15. [PubMed: 1774201]

McCarthy RT, TanPiengco PE. Multiple types of high-threshold calcium channels in rabbit sensory neurons: high-affinity block of neuronal L-type by nimodipine. J Neurosci 1992;12(6):2225–2234. [PubMed: 1318957]

McDonough SI, Boland LM, Mintz IM, Bean BP. Interactions among toxins that inhibit N-type and P-type calcium channels. J Gen Physiol 2002;119:313–328. [PubMed: 11929883]

Mergler S, Wiedenmann B, Prada J. R-type Ca^{2+}-channel activity is associated with chormogranin A secretion in human neuroendocrine tumor BON cells. J Membrane Biol 2003;194:177–186. [PubMed: 14502430]

Monsivais P, Rubel EW. Accommodation enhances depolarizing inhibition in central neurons. J Neurosci 2001;21:7823–7830. [PubMed: 11567073]

Newcomb R, Szoke B, Palma A, Wang G, Chen X, Hopkins W, Cong R, Miller J, Urge L, Tarczy-Hornoch K, Loo JA, Dooley DJ, Nadasdi L, Tsien RW, Lemos J, Miljanich G. Selective peptide antagonist of the class E calcium channel from the venom of the tarantula *Hysterocrates gigas*. Biochemistry 1998;37(44):15353–15362. [PubMed: 9799496]

Nishino E, Yamada R, Kuba H, Hioki H, Furuta T, Kaneko T, Ohmori H. Sound-intensity-dependent compensation for the small interaural time difference cue for sound source localization. J Neurosci 2008;28:7153–7164. [PubMed: 18614685]

Overholt EM, Rubel EW, Hyson RL. A circuit for coding interaural time differences in the chick brainstem. J Neurosci 1992;12(5):1698–1708. [PubMed: 1578264]

Parks TN, Rubel EW. Organization and development of brain stem auditory nuclei of the chicken: organization of projections from n. magnocellularis to n. laminaris. J Comp Neurol 1975;164(4): 435–448. [PubMed: 1206128]

Patil PG, de Leon M, Reed RR, Dubel S, Snutch TP, Yue DT. Elementary events underlying voltage-dependent G-protein inhibition of N-type calcium channels. Biophys J 1996;71:2509–2521. [PubMed: 8913590]

Randall A, Tsien RW. Pharmacological dissection of multiple types of Ca^{2+} channel currents in rat cerebellar granule neurons. J Neurosci 1995;15(4):2995–3012. [PubMed: 7722641]

Reid CA, Bekkers JM, Clements JD. Presynaptic Ca^{2+} channels: a functional patchwork. Trends Neurosci 2003;26:683–687. [PubMed: 14624853]

Reyes AD, Rubel EW, Spain WJ. Membrane properties underlying the firing of neurons in the avian cochlear nucleus. J Neurosci 1994;14(9):5352–5364. [PubMed: 8083740]

Rubel EW, Parks TN. Organization and development of brain stem auditory nuclei of the chicken: tonotopic organization of n. magnocellularis and n. laminaris. J Comp Neurol 1975;164:411–433. [PubMed: 1206127]

Rubel, EW.; Parks, TN. Organization and development of the avian brain-stem auditory system. In: Edelman, GM.; Einar Gall, W.; Maxwell Cowan, W., editors. Brain function. New York: John Wiley & Sons; 1988. p. 3-92.

Saunders JC, Coles RB, Gates GR. The development of auditory evoked responses in the cochlea and cochlear nuclei of the chick. Brain Res 1973;63:59–74. [PubMed: 4764322]

Sidach SS, Mintz IM. Low-affinity blockade of neuronal N-type Ca channels by the spider toxin ω-Agatoxin-IVA. J Neurosci 2000;20(19):7174–7182. [PubMed: 11007873]

Tang Z, Gao H, Lu Y. Control of a depolarizing GABAergic input in an auditory coincidence detection circuit. J Neurophysiol. 2009In Press

Urbano FJ, Piedras-Renteria ES, Jun K, Shin H, Uchitel OD. Altered properties of quantal neurotransmitter release at endplates of mice lacking P/Q-type Ca^{2+} channels. Proc Natl Acad Sci USA 2003;100(6):3491–3496. [PubMed: 12624181]

Wu LG, Borst JG, Sakmann B. R-type Ca^{2+} currents evoke transmitter release at a rat central synapse. Proc Natl Acad Sci USA 1998;95:4720–4725. [PubMed: 9539805]

Wu LG, Westenbroek RE, Borst JG, Catterall WA, Sakmann B. Calcium channel types with distinct presynaptic localization couple differentially to transmitter release in single calyx-type synapses. J Neurosci 1999;19(2):726–736. [PubMed: 9880593]

Yang L, Monsivais P, Rubel EW. The superior olivary nucleus and its influence on nucleus laminaris: a source of inhibitory feedback for coincidence detection in the avian auditory brainstem. J Neurosci 1999;19:2313–2325. [PubMed: 10066281]

Ye JH, Zhang J, Xiao C, Kong JQ. Patch-clamp studies in the CNS illustrate a simple new method for obtaining viable neurons in rat brain slices: glycerol replacement of NaCl protects CNS neurons. J Neurosci Methods 2006;158:251–259. [PubMed: 16842860]

Young SR, Rubel EW. Frequency-specific projections of individual neurons in chick brainstem auditory nuclei. J Neurosci 1983;3(7):1373–1378. [PubMed: 6864252]

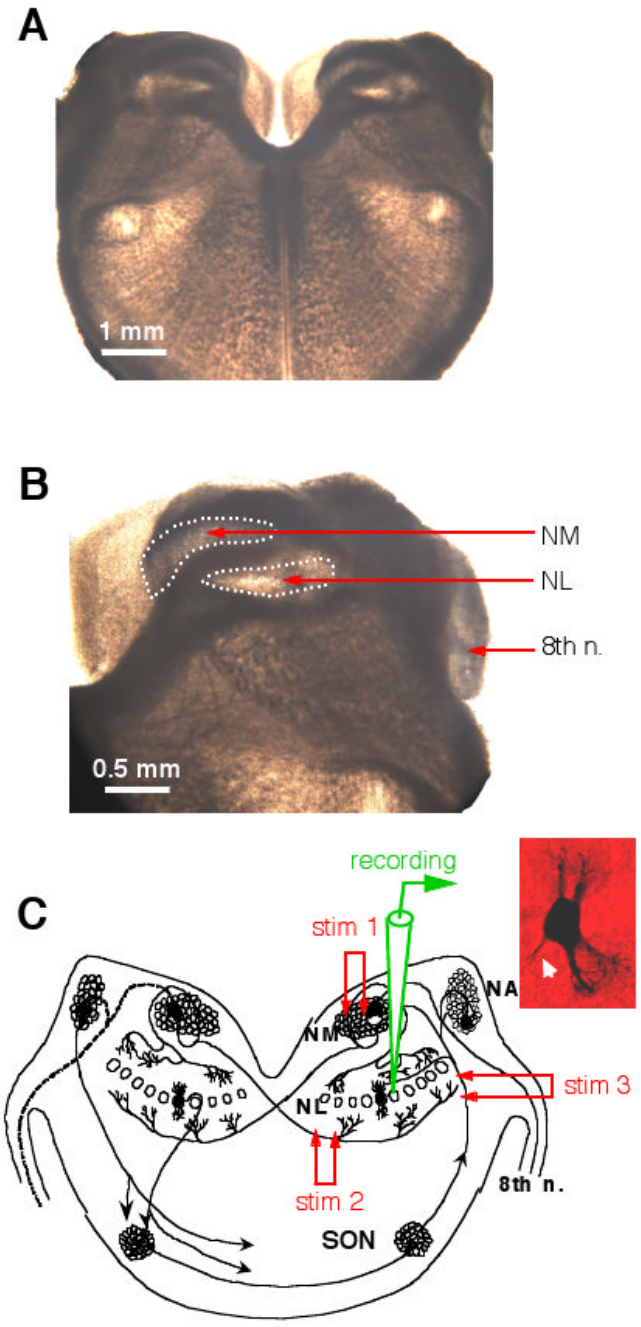

Figure 1.

Experimental preparation. ***A and B:*** Photographs (bright field illumination) of a chicken brainstem slice (300 μm in thickness). No staining was performed. The stump of the 8th nerve, the nucleus magnocellularis (NM) and nucleus laminaris (NL) can be easily identified. ***C***: A schematic diagram showing the time-coding circuits in the avian auditory brainstem. The auditory nerve innervates the cochlear nucleus angularis (NA) and the NM. Neurons in the NM send bilaterally segregated excitatory projections to the NL. Stimulation electrode 1 (stim 1) was placed in the ipsilateral NM to activate the dorsal excitatory input to the NL, and stim 2 on the fibers ventral and medial to the NL to activate the excitatory input from the contralateral NM. Neurons in the NL receive GABAergic inputs primarily from the ipsilateral superior

olivary nucleus (SON). Stim 3 was placed on the SON fibers to activate the GABAergic pathway. The inset shows the morphology of one NL neuron revealed by biocytin staining (axon indicated by the white arrow).

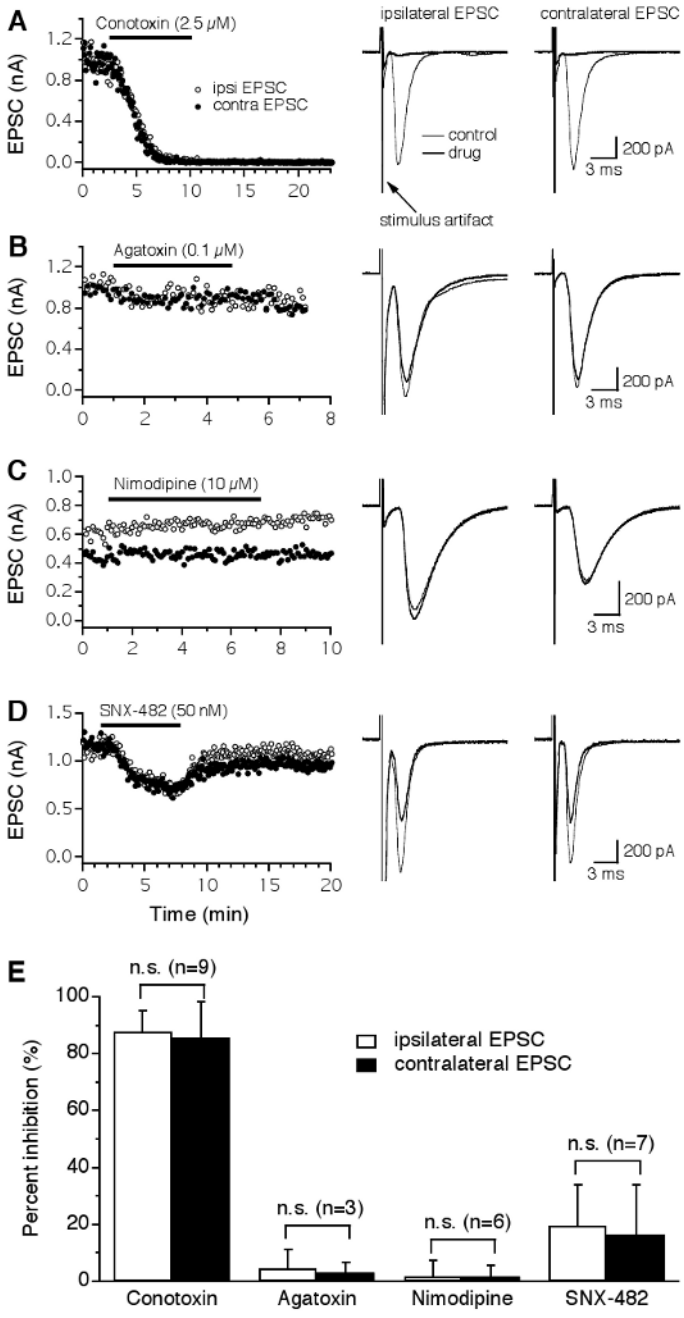

Figure 2.

Glutamatergic transmission in the NL is predominantly triggered by Ca^{2+} entry through N-type VGCCs. ***A***: Both the ipsilateral (open circles) and the contralateral (filled circles) EPSCs recorded from the same NL neuron were largely and irreversibly blocked by the N-type blocker ω-Conotoxin-GVIA (ω-CTx-GVIA, 2.5 μM), with nearly identical time courses. Averaged traces under control (thin traces) and drug (thick traces) conditions are shown on the right. Stimulus artifacts are truncated for clarity. ***B-C***: No inhibition of EPSCs was produced by the P/Q-type blocker ω-Agatoxin-IVA (ω-Aga-IVA, 0.1 μM) or the L-type blocker nimodipine (10 μM). ***D:*** A small and reversible inhibition of the EPSCs by the R-type blocker SNX-482 (50 nM) was observed. The different time courses of the EPSCs observed in the sampled

neurons may be due to different locations of the neurons along the tonotopic frequency axis. ***E***: Summary of the effects of different VGCC blockers on EPSCs of NL neurons. ω-CTx-GVIA inhibited the ipsilateral and the contralateral EPSCs by 88% and 86%, respectively. Blockers for P/Q- and L-type VGCCs had no effects on EPSCs. SNX-482 produced a small inhibition with a large variation among cells. No differences in the percent inhibition by either drug were detected between the ipsilateral and the contralateral EPSCs. Error bars represent standard deviations. n.s.: non-significant (paired t-test, $p > 0.05$; the number of cells is indicated in parentheses).

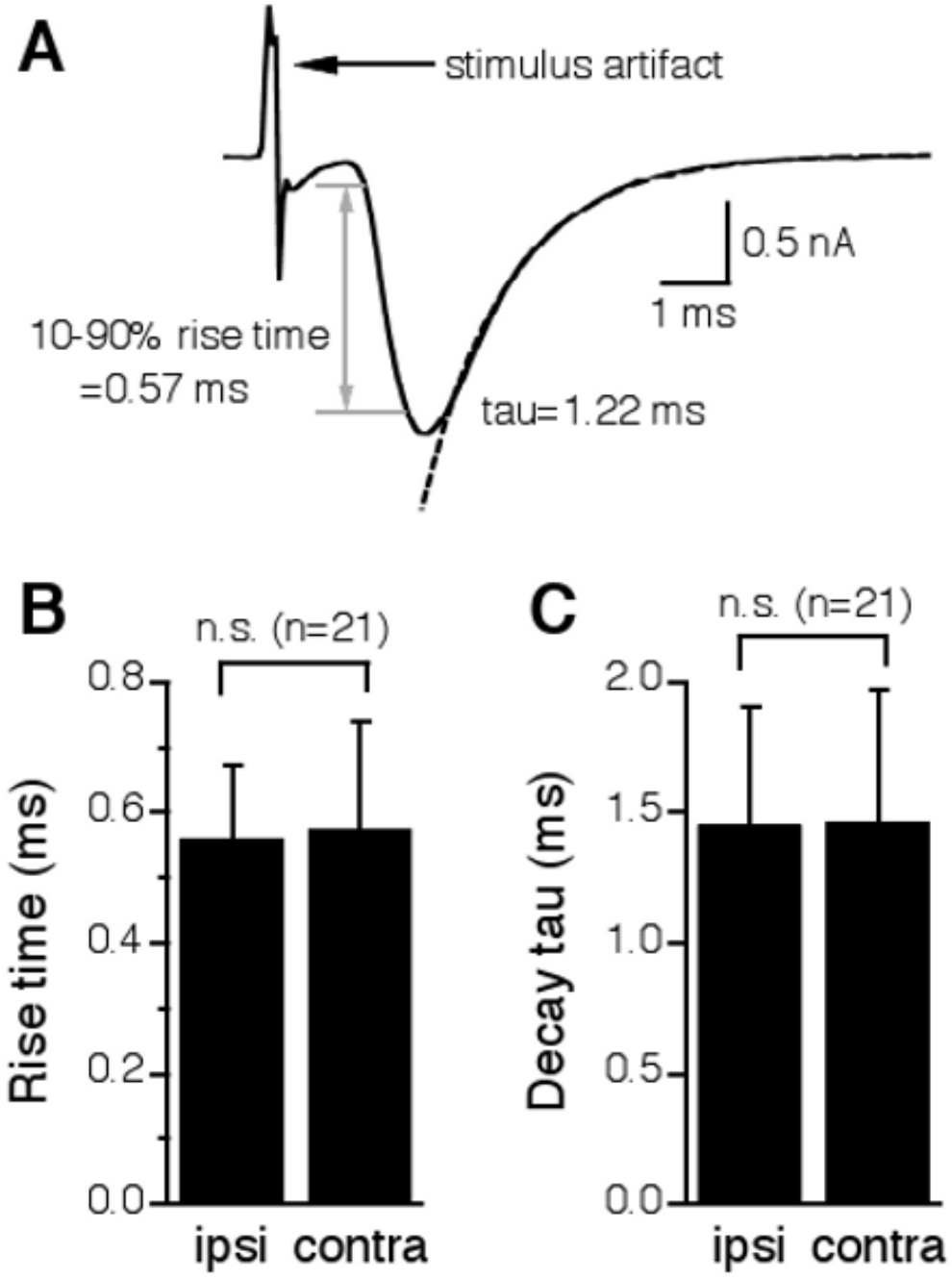

Figure 3.

The ipsilateral and the contralateral EPSCs in the same NL neurons have nearly identical kinetics. ***A***: One representative EPSC showing the measurements of the 10-90% rise time and the decay time constant (tau). The time period that takes for the EPSC to change from 10% to 90% of its peak value is defined as the 10-90% rise time (indicated by the gray lines and the double-head arrow). The decay tau was measured by fitting a single exponential curve (dashed line) to the portion from the peak of the EPSC to the baseline. ***B and C***: A paired t-test revealed no statistical differences between the ipsilateral and the contralateral EPSCs in either 10-90% rise time or decay tau.

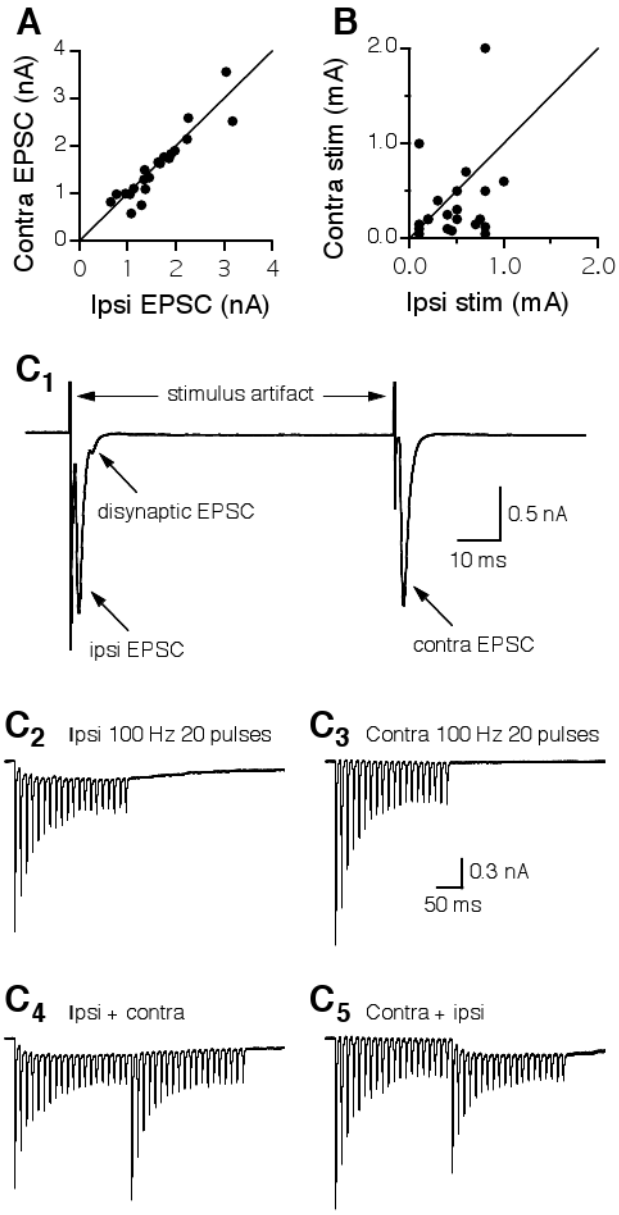

Figure 4.

Independence of the electrical stimulations eliciting the ipsilateral and the contralateral EPSCs in individual NL neurons. ***A***: EPSCs with similar peak amplitudes were intentionally elicited in each neuron by adjusting the stimulus intensities. Consequently, when the peak amplitude of the contralateral EPSC was plotted against that of the ipsilateral EPSC, the data points fell on or were very close to the line indicating equivalence. The distribution of the stimulus intensities, however, is much more scattered (***B***). ***C1***: Ipsilateral and contralateral EPSCs elicited by two single electrical shocks delivered at an interval of 75 ms. A disynaptic EPSC was observed in the recordings of the ipsilateral, but not the contralateral EPSCs. ***C2***: EPSCs elicited by a train of synaptic stimulation (100 Hz, 20 pulses) to the ipsilateral input showed synaptic depression and temporal summation. ***C3***: EPSCs elicited by the same train stimulation (100 Hz, 20 pulses) to the contralateral input showed synaptic depression but little summation. ***C4***: The ipsilateral train stimulation was followed by the contralateral train stimulation. The

contralateral EPSCs that follow the ipsilateral EPSCs showed a similar profile to that elicited by the contralateral stimulation alone, and vice versa (***C5***). Stimulus artifacts in C_2-C_5 are blanked.

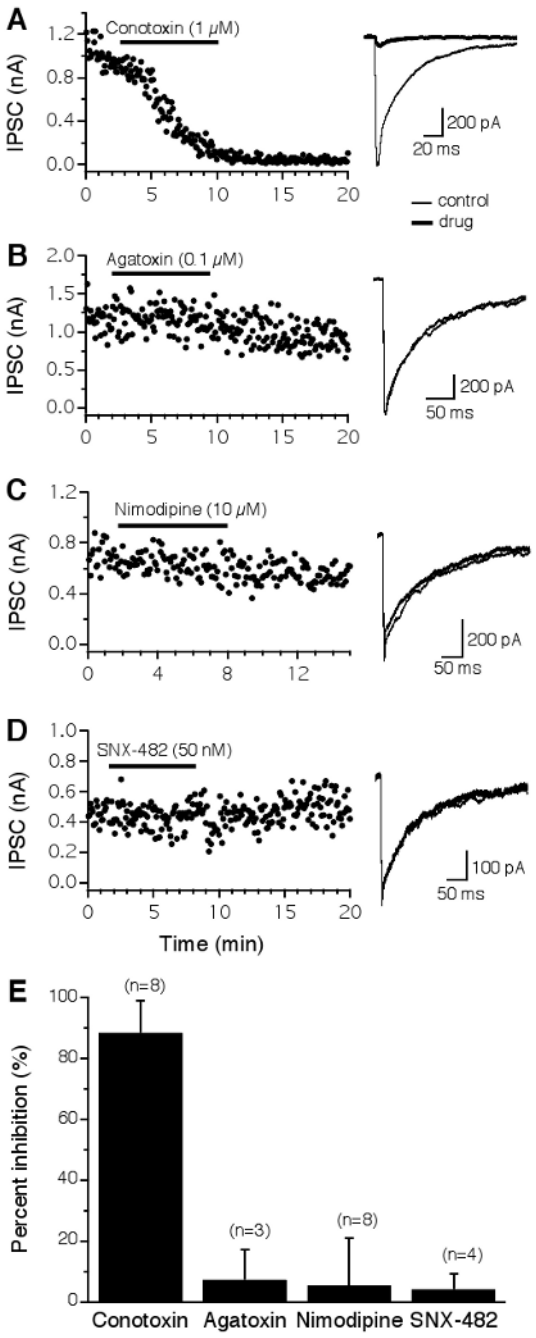

Figure 5.

GABAergic transmission in the NL is almost exclusively triggered by N-type VGCCs. ***A***: IPSCs were almost completely and irreversibly blocked by ω-CTx-GVIA (1 μM). ***B-D:*** Little or no inhibition by blockers for non-N-type channels. ***E***: Summary of the effects of different VGCC blockers on IPSCs of NL neurons. See Figure 2 for a detailed legend.

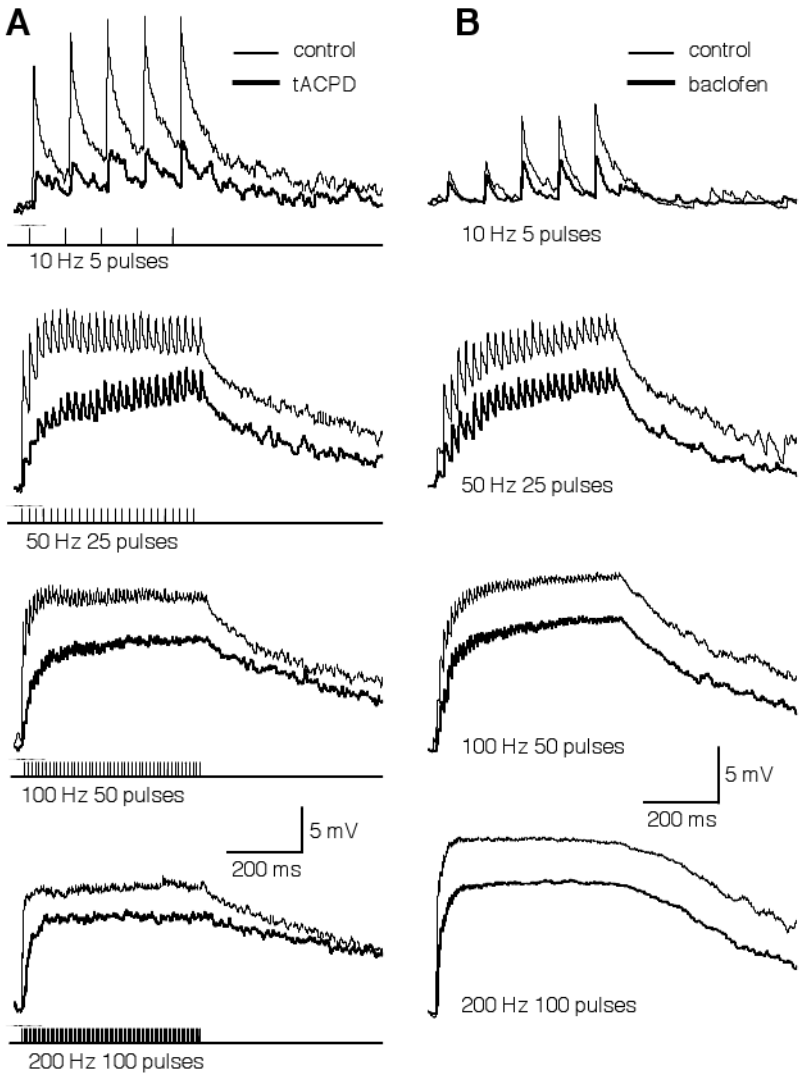

Figure 6.

The temporal profile of GABA-induced IPSPs in NL neurons is not altered by modulation mediated by mGluRs (***A***) or $GABA_B$ receptors (***B***). GABAergic IPSPs were evoked by synaptic stimulations (duration of 500 ms) at different frequencies, under control (thin traces) and drug (thick traces) conditions (***A***: 100 μM tACPD, a non-specific mGluR agonist; ***B:*** 100 μM baclofen, a $GABA_BR$ agonist). Due to a high intracellular Cl^- concentration in NL neurons (Tang et al., 2009), activation of the GABAergic pathway gives rise to membrane depolarization up to about 15 mV. Discrete IPSPs were observed in response to a low frequency stimulation (10 Hz). Temporal summation of IPSPs occurred at higher frequencies. Activation of either mGluRs or $GABA_B$ receptors substantially reduced the amplitude of the IPSPs, but maintained a depolarizing plateau at high stimulation frequencies. Stimulation artifacts are blanked for clarity. The resting membrane potentials of the neurons were -65 (***A***) and -61 mV (***B***), respectively.